Meteorological and geological influences on icing dynamics in subarctic Northwest Territories, Canada

P.D. Morse[1] & S.A. Wolfe[1,2]
[1]*Geological Survey of Canada, Natural Resources Canada, Ottawa, Ontario, Canada*
[2]*Department of Geography and Environmental Studies– Carleton University, Ottawa, Ontario, Canada*

ABSTRACT
In this study, we test the significance of identified meteorological forcing variables against a long-term dataset of icing dynamics and distribution developed for the Yellowknife region, Northwest Territories. Overall, 28% of icing density interannual variation is explained by winter warming periods (≥5°C) and autumn rainfall. Interannual icing density variation and significant meteorological forcing variables differ among ecoregions where varied geological permafrost conditions influence the hydrological regime.

RÉSUMÉ
Dans cette étude, un ensemble de données à long terme qui représente la distribution et la dynamique de formation de couches de glace dans la région près de Yellowknife, Territoires du Nord-Ouest, a été utilisé pour tester l'influence de variables de conditionnement météorologique préalablement identifiées. En général, 28% de la variation interannuelle de la densité de couches de glace est attribuée aux réchauffement hivernaux (>5°C) et aux précipitations automnales. Les variations interannuelles de la densité des couches de glace et les variables significatives de conditionnement météorologique varient d'une écorégion à l'autre, où différents contextes géologiques et de pergélisol influencent le régime hydrologique.

1 INTRODUCTION

Icings (a.k.a. aufeis, naled) are sheet-like masses of layered ice that form during the winter by freezing of successive flows of water on the ground surface, or on top of river or lake ice (ACGR 1988). Common throughout the northern hemisphere (Yoshikawa et al. 2007), icing development has been linked to periodic increases in winter air temperature (winter warming periods) (Kane 1981), high autumn precipitation (Hall and Roswell 1981), and low early-winter snow fall (Carey 1973). Icings are a geohazard, negatively impacting the performance of infrastructure where overflow encroaches on roadways or buildings, or damaging infrastructure if extensive springtime flooding is induced (Carey 1973). Controlled by local and regional factors, icings are spatially recurrent, but not annually, nor to the same extent. Thus, long-term datasets of icing dynamics and distribution are required to improve process studies and identify potential terrain hazards.

In this paper we assess how identified local and regional factors affect long-term icing dynamics in the subarctic. We hypothesize that icing area varies over time according to meteorological forcing variables, with spatial variation due to hydrological setting moderated by geological conditions. We test this hypothesis by examining the influence of autumn rainfall, early-winter snowfall and air temperature, total winter snowfall, and frequency of sporadic winter warming periods on interannual variation of icing area. Divided into four ecologically and geologically distinct ecoregions (Fig. 1) (ECG 2007; 2008), hydrological conditions in the study area are representative of much of the subarctic.

Figure 1. Ecoregions within the Northwest Territories study area showing shaded relief. Figure 2 image extent is outlined.

2 BACKGROUND

2.1 Icings

Icing occurrence and process dynamics are influenced by climate, hydrology, geology, permafrost, and topography

(Carey 1973; Kane 1981). Conditions most favourable for icing formation are severe continental climate, cold winters with low snow cover, the presence of groundwater springs or unfrozen, water-bearing taliks, and highly permeable materials such as sand or gravel deposits, organic matter, or karst terrain (Romanovskii et al. 1996). Interannual variation of icing activity reportedly relates to the autumn rainfall (Carey 1973; Hall and Roswell 1981), and the extent of icing development may vary inversely with snow cover (Carey 1973; Yoshikawa et al. 1999).

Overflow events are driven by a rise in hydrostatic head associated with winter warming periods (Kane 1981). Yoshikawa et al. (1999) noted the frequency of winter warming periods of 15°C d^{-1} seemed related to icing development at Caribou-Poker Creeks Research Watershed, AK, where Kane (1981) identified the pore water pressure–temperature relation. The process underpinning this relation is unknown, but repeated overflow events throughout the winter increase the ice thickness, and by the end of the cold season the channel and adjacent floodplain may fill completely with ice.

2.2 Study Area

The study area, delimited by the extent of one Landsat satellite scene (WRS-2 Path 47, Row 16; 21887 km^2 land area), is in subarctic Northwest Territories and includes Yellowknife (Fig. 1). The regional climate is strongly continental, with cold winters (-25.6°C January mean temperature) and relatively warm summers (17.0°C July mean temperature). Nearly 76% of the annual precipitation (289 mm) falls as rain from May to November, with scant snowfall over the winter months. Due to higher autumn rainfall since 1997, there has been an increase in the frequency of autumn runoff events and increased winter streamflow (Spence et al. 2011, 2014). Beginning in late-September, snow accumulates steadily throughout the winter until April when the normal month-end snow depth is 0.37 m. Snowmelt is largely complete by the end of April, with total ablation by the end of May.

The study area, located in the extensive discontinuous permafrost zone (Heginbottom et al. 1995), is divided by four ecoregions of the Great Slave geological district (Fig. 1) (ECG 2007, 2008), which from south to north are: (i) the Plain High Boreal (PHB); (ii) the Lowland High Boreal (LHB); (iii) the Upland High Boreal (UHB); and (iv) the Upland Low Subarctic (ULS).

PHB (5418 km^2) is characterized by a gentle, dome-shaped topography, underlain by horizontally bedded dolomite, limestone and sandstone of Cambrian to Devonian age, with an average elevation of 200 m asl Frequently burned, this dry, well drained plain, capped by washed till through the centre of the region, is forested by extensive young jack pine (Pinus banksiana) stands and white spruce (Picea glauca) that grow adjacent to small streams and wetlands. The karst topography with numerous shallow marl ponds is unique in the Northwest Territories (ECG 2007).

LHB (4042 km^2) is a nearly-level Precambrian granitoid bedrock plain with extensive, discontinuous wave-washed tills, glaciolacustrine and lacustrine deposits, and glaciofluvial materials occurring between outcrops and in bedrock fractures (Kerr and Wilson 2000), where wetlands are common. Elevations range from about 160 to 200 m asl, with the northern boundary coinciding with the limit of extensive lacustrine sediments (Stevens et al. 2012). Permafrost, associated with those sediments, is more extensive in LHB than the other ecoregions (Morse et al. in press). A wide array of forest types occur, ranging from black spruce (Picea mariana) dominant to pure paper birch stands (Betula papyrifera). Jack pine and aspen (Populus tremuloides) forests occur on well drained areas.

In contrast, UHB (8215 km^2) is a gently southwest-sloping Precambrian sedimentary bedrock plain with few local promontories, and is dominantly overlain with thin discontinuous till veneers and scattered outwash deposits. Glacial Lake McConnell reached a maximum elevation of about 290 m asl, covering most of UHB, where elevations range from at least 200 to 300 m asl (Kerr and Wilson 2000). Consequently, thin, discontinuous deposits of wave-washed tills, glaciolacustrine sediments, and glaciofluvial materials occur in rock fractures and between outcrops, where the substrate is sufficiently thick for discontinuous black spruce and jack pine forests.

More rugged than the UHB, ULS (4211 km^2) ranges from gently rolling terrain, to rugged local hill systems, with several large lakes and rivers. Southwest sloping, this Precambrian granitoid bedrock upland with two broad plateaus ranges in elevation from about 275 to 450 m asl. Frost shattered bedrock blockfields dominate the landscape, with discontinuous till and sparse spruce and birch forests. Locally extensive outwash deposits occur, but are mainly to the east and north, whereas organic deposits are numerous but have a limited extent.

3 DATA AND METHODS

3.1 Icing Mapping

Morse and Wolfe (2014) developed a new semi-automated remote sensing technique to map icings in the subarctic, which is summarized as follows:

Icing distribution was mapped with Landsat satellite image data (TM, ETM+, and OLI sensors), which are advantageous because icings are clearly evident in images acquired following the snowmelt season (Fig. 2a) (Hall and Roswell 1981; Yoshikawa et al. 2007), the images cover large areas and are easy to obtain (http://glovis.usgs.gov/), and the 30-year archive enables long-term dataset generation. Late-spring images of sufficiently low cloud cover were available for 24 years. Following radiometric and geometric corrections, snow and ice were discriminated from soil, rock, and cloud cover with a Normalized Difference Snow Index (NDSI) (Hall et al. 1995) (Fig. 2b):

$$NDSI = (G - SWIR1) / (G + SWIR1) \quad (1)$$

where G and SWIR1 are green and shortwave infrared portions of the electromagnetic spectrum, respectively. Following Hall et al. (1995), 0.4 was selected as the threshold value for snow and ice (Fig. 2c); however, this

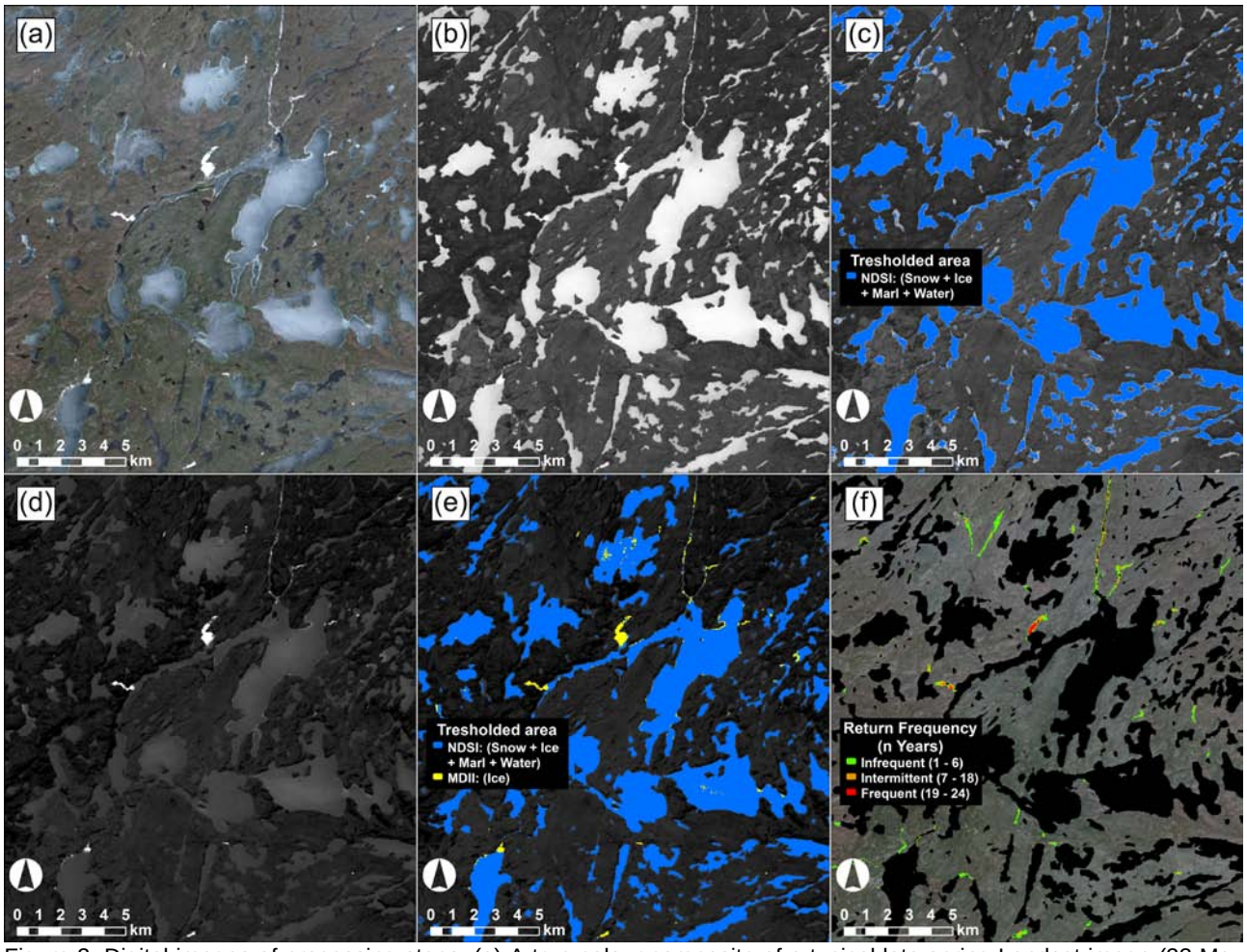

Figure 2. Digital images of processing steps: (a) A true colour composite of a typical late-spring Landsat image (23 May 2013) with several bright white icings visible (b) Normalized Difference Snow Index (NDSI); (c) Threshold NDSI values shown in blue; (d) Maximum Difference Ice Index (MDII); (e) Threshold MDII values shown in yellow; (f) The true color composite overlain by the total extent of icings mapped using the 24-year dataset, with the return frequency of each mapped pixel indicated, and lake and river ice removed by a black water mask.

threshold value did not exclude wet marl and shallow marl-bottomed lakes. Consequently, ice was extracted with an exaggerated basic difference index, the new Maximum Difference Ice Index (MDII) (Fig. 2d):

$$MDII = (G^2 - SWIR1^2). \quad (2)$$

MDII threshold values of 0.144 and 0.040 discriminate ice in scenes with and without snow, respectively (Fig. 2e). Following ice extraction, a water mask derived from a number of summer images was applied to remove river and lake ice, conservatively leaving only land-fast ice (Fig. 2f).

Icing activity was determined from the count of instances (years) when ice was present within the maximum aggregate extent of ice (Fig. 2f). Icings were classified according to return frequency as infrequent (1-6), intermittent (7-18), or frequent (19-24) on the 24-year dataset.

3.2 Assessment of Meteorological Forcing Variables

Daily average meteorological data available for Yellowknife airport from 1943 to 2014 (Environment Canada http://weather.gc.ca/) were compiled in order to determine the relative influence of autumn rainfall, early-winter snowfall and air temperature, and frequency of winter warming periods on icing dynamics, and to determine historical trends. Autumn rainfall was the sum of September-to-October events, early-winter snowfall was the October-to-December sum, and early-winter air temperature was the October-to-December mean. Warming period magnitudes were determined from the sum of consecutive daily increased air temperature. As the most influential magnitude of warming on icing variation is unknown, the frequency of warming periods (i.e. the frequency of events with a ≥5°C total increase in air temperature) was calculated for a range of magnitudes (1-15°C). Forward stepwise multiple-linear regressions were used to determine the influences of meteorological forcing variables on annual icing density.

4 RESULTS

4.1 Mapped Icings

A total of 5500 icings are mapped in the study area (Fig. 3). Satellite image date and cloud cover have little overall influence on interannual icing variation (Fig. 4a). It was impossible to quantitatively assess the mapping error against an independent measurement of icing area, as aerial photographs of the region are taken in mid-summer, as are most very-high resolution satellite images that also have limited coverage. Consequently, icing mapping results were assessed visually (though many of the icings mapped in 2013 and 2014 were confirmed via helicopter); the results were overlaid on image data where icings are visually distinguishable (Fig. 2a).

Visual inspection of all scenes with snow indicated icings are underestimated at the expense of overestimating snow. However, snow free images with a lower MDII threshold are not an overall improvement, because the increased ablation means that smaller icings may no longer be evident and the margins of larger icings have likely retreated. Because of the nature of icing dynamics and the timing of image acquisition each spring season, the relative number and area of icings is more important to this study than absolute values for comparative purposes. The broad agreement between icings mapped, observed, and visually assessed suggests icing dynamics were adequately captured for the purpose intended.

4.2 Icing Distribution and Dynamics

Variation of total icing extent (1985 to 2014) by ecoregion is shown in Figure 3, icing dynamics are statistically summarized in Table 1 and shown in Figure 4, and variation of annual icing extent by ecoregion is shown in Figure 5. The maximum extent of icings (86 km^2) indicates they affect 0.39% of the land (Fig. 3). Interannual variation of icing density ranges from a maximum (13×10^{-4} km^2 km^{-2}) in 2004 to a minimum (6×10^{-5} km^2 km^{-2}) just two years later (Fig. 5). Discrete icings range in size from 1800 m^2 to 4 km^2, (Fig. 4b). The majority (93%) of icings are infrequent and return frequency generally increases with icing size (Fig. 4c, Table 1).

Icing distribution patterns, densities, and dynamics vary by ecoregion (Figs. 3, 4, and 5). The highest cumulative total icing count (3214), density (0.88%) and area (48 km^2) of any ecoregion occurred at PHB (Fig. 3). The high density can be attributed mainly to extensive icing development in 2002 and 2004 (Fig. 5). However, annual icing density ranged to as low as 1×10^{-5} km^2 km^{-2} (Fig. 5). Icings are small but numerous (Fig. 4), with intermittent or frequent ice cumulatively constituting only 3.5% of icings and 2.3% of the total icing area.

At LHB, 98% of the icings are infrequent, none are frequent, and consequently LHB has the lowest cumulative total icing area (3 km^2) and total icing density (0.07%) of any ecoregion with only 275 icings mapped (Figs. 3 and 4, Table 1). The degree of interannual variation is subdued compared with PHB, though the most extensive icing development at LHB also occurred in 2004 (Fig. 5).

UHB has the highest icing count (1175) and total icing area of 19 km^2 of the shield bedrock ecoregions, yielding a 0.23% density (Figure 4). Annual icing densities range from a minimum 3×10^{-5} km^2 km^{-2} in 2012 to 7×10^{-4} km^2 km^{-2} in 2004 (Fig. 5). Icing return frequencies are up to 88% (Fig. 4c), but 91% of icings are infrequent (Table 1).

At ULS the count (836) and area (17 km^2) are less than at UHB, but the icings are the most densely distributed (0.40% overall density) and active in the Taiga Shield ecoregions (Figs. 3 and 5). In stark contrast to other ecoregions, about 15% of the icings at ULS are intermittent, and 2.4% re-develop almost every year (Table 1). The average icing size is also much larger than at other ecoregions north of Great Slave Lake (Fig. 4b).

4.3 Meteorological Forcings on Interannual Icing Variation

Regression statistics for significant meteorological forcings on icing dynamics are shown in Table 2. Overall, winter warming periods (≥5°C) and autumn rainfall explain about 28% of interannual variation of icing density, with warming periods making a somewhat greater contribution.

Like interannual variations of icing density (Fig. 5), significant meteorological forcing variables are not coincident amongst ecoregions (Table 2). At PHB only warming periods (≥6°C) enter the regression, explaining 14% of interannual variation of icing density. Winter warming periods (≥8°C) are also the only significant forcing at LHB, but they significantly explain 24% of the interannual variation. At UHB warming periods (≥5°C) are also dominant with autumn rainfall as a secondary determinant, together explaining 31% of icing variation. Further north at ULS, autumn rainfall and an inverse relation to the early-winter mean air temperature explain 34% of interannual icing density variation.

5 DISCUSSION

5.1 Geological Influences on Icing Dynamics

Icings vary substantially among ecoregions in relation to geological setting (Figs. 3, 4, and 5). Limestone and dolomite bedrock with karst topography and hydrology, beneficial to icing development (Romanovskii et al. 1996), defines PHB. Consequently, many icings there develop in the vicinity of springs that feed the numerous marl ponds. The flat terrain allows for potentially large icings because overflow may not be confined to a valley. Accordingly, even infrequent icings may be extensive, diminishing the strength of the relation between size and return frequency, as compared to icings that develop within the Precambrian Shield (Fig. 4c). However, there are distinct differences within the Shield bedrock region. Low relief, thick fined-grained deposits, and extensive permafrost at LHB likely limit the occurrence and discharge from springs, and thus icing activity. Icings are likely more numerous at UHB than at LHB because surficial deposits are thin and more discontinuous, and permafrost is less

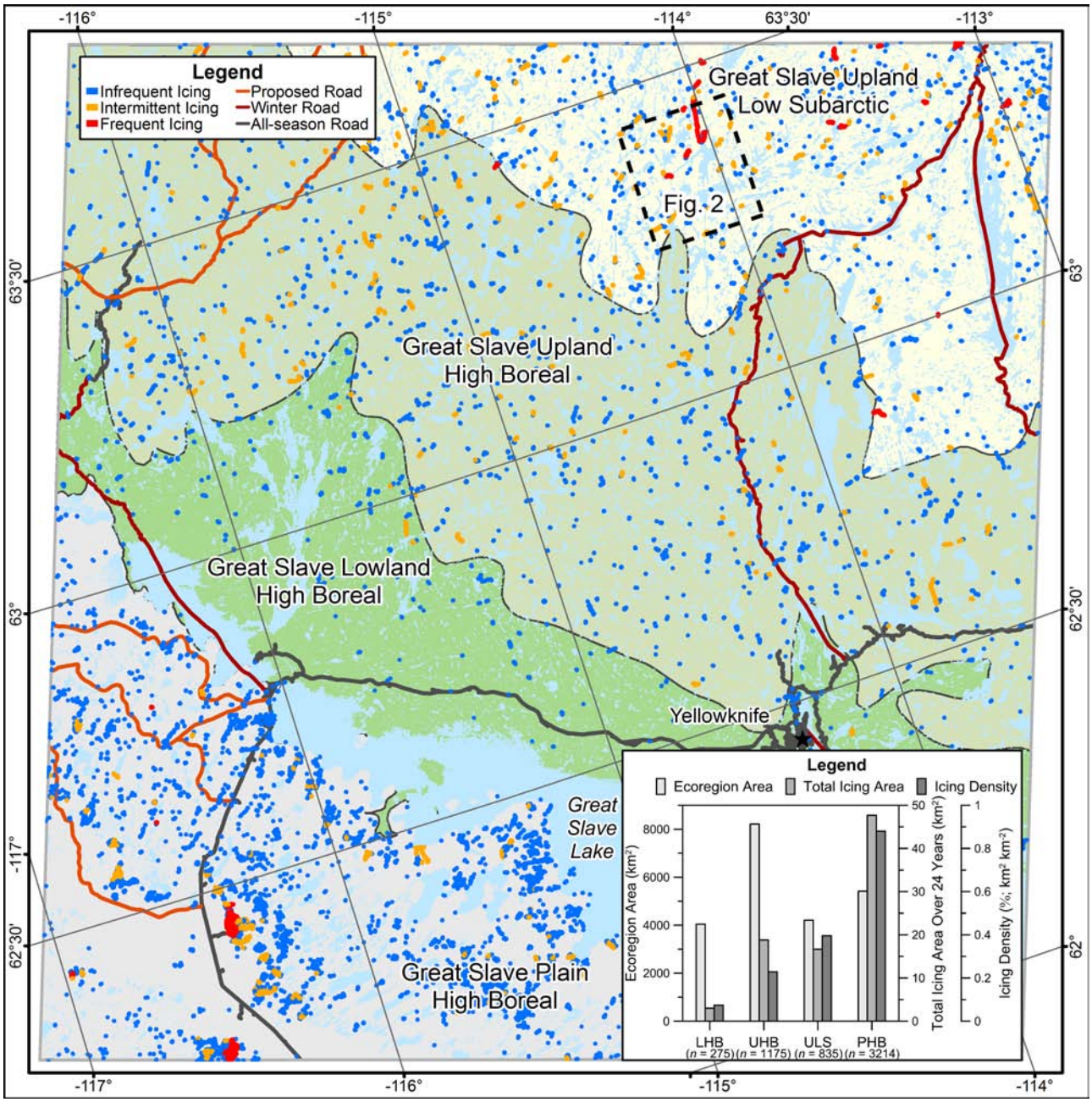

Figure 3. Total distribution of infrequent (1-6 returns), intermittent (7-18 returns), and frequent (19-24 returns) in the Great Slave region digitally mapped from Landsat data (1985 to 2014) for Lowland High Boreal (LHB), Upland High Boreal (UHB), Upland Low Subarctic (ULS), and Plains High Boreal (PHB) ecoregions, with an inset summarizing ecoregion area, total icing area, and total icing density. Figure 2 image extent is indicated.

Table 1. Percentage of icings distributed among Infrequent (1-6), Intermittent (7-18), and Frequent (19-24) return frequency classes for Lowland High Boreal (LHB), Upland High Boreal (UHB), Upland Low Subarctic (ULS), and Plains High Boreal (PHB) ecoregions (counts indicated in brackets).

Return Frequency	Overall (5500)	PHB (3214)	LHB (275)	UHB (1175)	ULS (836)
Infrequent	93.3 (5131)	96.5 (3102)	97.8 (269)	91.1 (1071)	82.4 (689)
Intermittent	6.2 (340)	3.2 (104)	2.2 (6)	8.8 (103)	15.2 (127)
Frequent	0.5 (29)	0.3 (8)	-	0.1 (1)	2.4 (20)

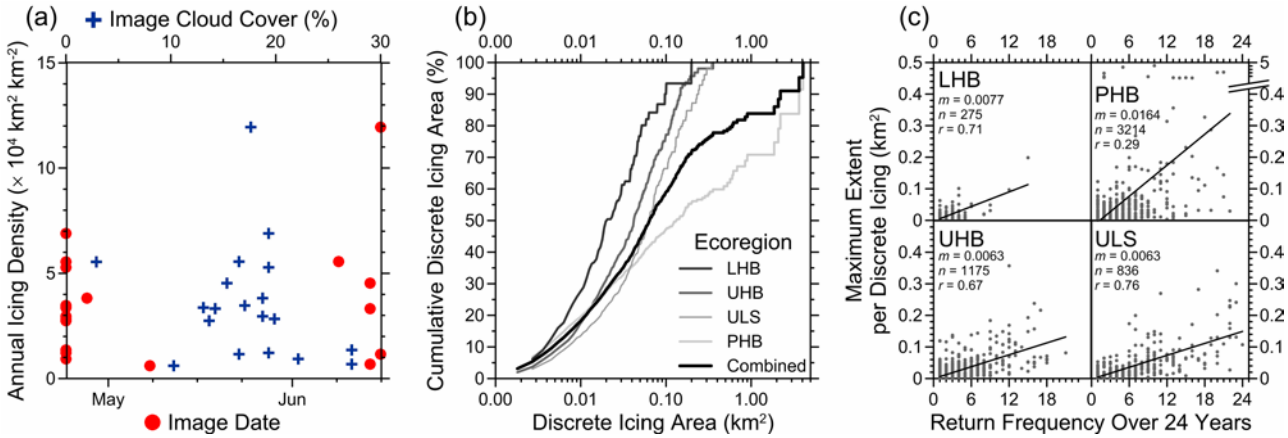

Figure 4. Icing dynamics for Lowland High Boreal (LHB), Upland High Boreal (UHB), Upland Low Subarctic (ULS), and Plains High Boreal (PHB) ecoregions: (a) Icing density versus satellite image acquisition date and percent cloud cover; (b) Cumulative discrete icing area versus discrete icing size. (c) Relations between maximum extent discrete icings (n = count) versus return frequency (m is the slope of the linear regression and r is the correlation coefficient).

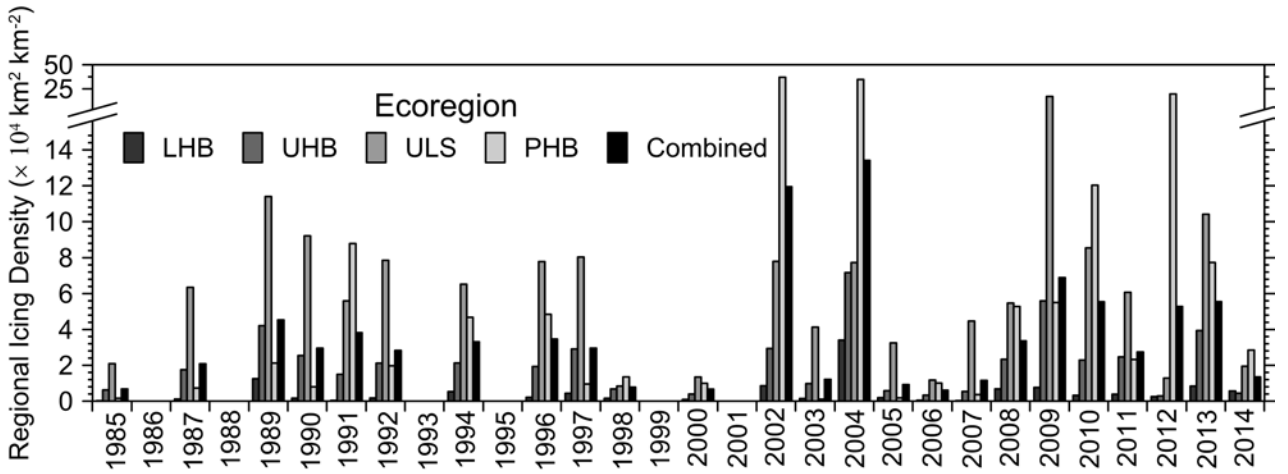

Figure 5. Interannual variation of icing density, 1985 to 2014, for Lowland High Boreal (LHB), Upland High Boreal (UHB), Upland Low Subarctic (ULS), and Plains High Boreal (PHB) ecoregions, determined from Landsat satellite images.

Table 2. Beta coefficient (β), adjusted coefficient of determination (Adjusted R^2), and significance (p) statistics for forward stepwise multiple-linear regression models of interannual variation of icing density forced by autumn rainfall, early winter snowfall and mean air temperature, and periodic warming events that remained in the model at the 0.05 level of significance, according to overall study region and Lowland High Boreal (LHB), Upland High Boreal (UHB), Upland Low Subarctic (ULS), and Plains High Boreal (PHB) ecoregions.

Model Components	Overall	PHB	LHB	UHB	ULS
Total rainfall (mm), Sep. To Oct. (β)	0.40			0.43	0.53
Total early-winter snowfall (cm), Oct. to Dec. (β)					
Mean air temperature (°C), Oct. to Dec. (β)					-0.44
Count of air temperature increases, >=5°C (β)	0.54			0.56	
Count of air temperature increases, >=6°C (β)		0.42			
Count of air temperature increases, >=7°C (β)					
Count of air temperature increases, >=8°C (β)			0.53		
Adjusted R^2	0.28	0.14	0.25	0.31	0.34
p	0.012	0.041	0.008	0.007	0.005

extensive. The configuration of basins in the exposed shield leads to a hydrology defined by a spill-and-fill regime (Spence and Woo 2003), with icings confined to valleys in contrast to PHB. Compared to UHB, the landscape at ULS is dominantly exposed, broken bedrock with plateaus covered by bouldery till veneers and sandy

to gravelly outwash deposits that are highly permeable, which promotes icing development (Romanovskii et al. 1996), and may account for the higher icing density. Indeed, Veillette and Thomas (1979) observed icings resulting from groundwater flowing through taliks present in coarse-grained glaciofluvial deposits in the District of Keewatin, NT, where permafrost is continuous.

5.2 Meteorological Influences on Icing Dynamics

Our findings (Table 2) confirm field observations made by others that icing development is related to winter warming periods (Kane 1981) and autumn rainfall (Hall and Roswell 1981), but here we show that the regional air temperature regime is the dominant overall driver of icing dynamics, with autumn rainfall of generally less importance. The most significant air temperature effect relates to the frequency of warming periods with a minimum 5°C rise in temperature. The winter of 2003-2004 exhibited the highest icing densities of any year (Fig. 5), and it had second highest count of warming periods ≥5°C and the highest counts of warming periods ≥6, 7, or 8°C. Icing counts in 2009 were also high in most regions (Fig. 5), with an average of 24 warming periods (≥5°C), but autumn 2008 was the wettest autumn with more than double the 48 mm average autumn rainfall.

However, under a similar climate, the hydrological regime varies throughout the region, likely due to different geology, topography, and permafrost conditions that modify hydrological conditions. At PHB, the limestone and dolomite bedrock create a karst hydrology that is substantially different than the spill-and-fill hydrology of shield bedrock (Spence and Woo 2003). This likely eliminates the importance of autumn rainfall and reduces the influence of the air thermal regime as the hydrology is not as physically constrained to surface waters as with spill-and-fill hydrology. Autumn rainfall is also not significant at LHB, where the population of icings (springs) is relatively low compared to the other ecoregions. This is likely due to a lesser spill-and-fill hydrological regime resulting from past basin infilling by sediment causing generally low relief. There may be additional hydrological restrictions due to permafrost that is more extensive locally than at the other ecoregions, as it occurs within the ecozone-defining widespread lacustrine deposits (Morse et al. in press).

At UHB, winter warming periods and autumn rainfall were both significant determinants of icing dynamics. Autumn rainfall entered the model likely because this ecoregion is typified by the spill-and-fill hydrological regime (Spence and Woo 2003). At UHB, compared with LHB, numerous lake basins are less infilled by sediment (Stevens et al. 2012). Because of low precipitation to evaporation ratios (Spence and Rouse 2002), summer storage deficits accumulate that prevent a basin runoff response until about 100 mm of rainfall has fallen between mid-July and the end of October (Spence et al. 2011, 2014). Thus, autumn rainfall is an important driver of early-winter baseflow and therefore icing dynamics.

Further north at ULS, interannual variation of icing density is related directly to autumn rainfall and inversely to the early-winter mean air temperature. Though larger basins with larger lakes attenuate the influence of autumn rainfall on early-winter baseflow in streams (Spence et al. 2011), the spill-and-fill regime dominates the hydrology and the rainfall signal is still present. However, within the ULS portion of the study area there is a relatively high concentration of large rivers that have generally more winter streamflow, which is indicated by the highest icing return frequencies and icing density compared to UHB and LHB (Figs. 3, 4, and 5, Table 1). It may be that with high winter streamflow, relatively cold early-winter conditions are important because a more extensive freeze must occur to create a stable, continuous ice cover. It is not apparent why winter warming periods were not significant in this ecoregion. Perhaps with generally higher stream flow and thus pore water pressure, overflow may be more continuous, requiring little influence by warming periods. Alternatively, the ice thickness may be important because the relation between pore water pressure and air temperature becomes increasingly disassociated as ice thickness increases (Kane 1981). Therefore, as the icings at UHB and ULS are both confined to valleys, the larger and hence thicker icings at ULS may not be affected to the same degree by periodic warming.

It is important to note that meteorological relations established in this study depend upon data from a single climate station. The climate is regionally consistent (Morse et al. in press), but local-scale factors that may be very important to icing dynamics at a particular location are not captured, such as the influence of local snow depth variation due to drifting.

6 SUMMARY AND CONCLUSIONS

Overall, 5500 icings are mapped from 24 late-spring Landsat images of the Great Slave region around Yellowknife. These data, generated using a new semi-automated approach, enable the first ever analysis of regional icing distribution and dynamics produced in Canada, and establish a baseline for winter hydrological variability in the region against which future icing conditions, under changing climate and precipitation regimes, may be compared. These data also provide important geoscience information required to assess terrain risks to northern transportation infrastructure, and may guide route selection for future transportation corridors.

Icing size is directly related to return frequency. Over 93% of icings are infrequent, occurring 25% of the time or less. Icing area varies substantially and among ecoregions because of differing geology, topography, and permafrost conditions that constrain the hydrological regime and the extent to which overflow may spread at the surface. Limestone and dolomite bedrock terrain promotes numerous icings via karst drainage networks. Where bedrock is capped by thick unconsolidated deposits with permafrost, springs are likely limited and icings are uncommon. The greatest density of icings in the study region north of Great Slave Lake occurs where the extensively exposed granitoid Precambrian Shield bedrock is highly fractured (and may be permafrost free), which may permit relatively high hydraulic connectivity

between numerous recharge and discharge zones.

Icing area and count, which varied considerably from year to year, is related to the frequency of winter warming periods and the amount of autumn rainfall preceding freeze-up. However, icing dynamics and significant meteorological forcing variables are not coincident among ecoregions due to differences in hydrological regimes among the ecoregions.

ACKNOWLEDGEMENTS

Derived annual icing data are available in Morse and Wolfe (2014). This work was conducted under the Great Slave – TRACS (Transportation Risk in the Arctic to Climate Sensitivity) program of the Geological Survey of Canada, Natural Resources Canada. Thanks to F. Hassan for downloading Landsat data. This is ESS contribution #20150062.

REFERENCES

Associate Committee on Geotechnical Research (ACGR). 1988. Canadian Glossary of Permafrost and Related Ground-Ice Terms, *Technical Memorandum No. 142*, National Research Council of Canada, Ottawa, ON.

Carey, K.L. 1973. Icings Developed from Surface Water and Ground Water, *Cold Regions Science and Engineering Monograph 111-D3*, U.S. Army Cold Regions Research and Engineering Laboratory, Hanover, NH, USA.

Ecosystem Classification Group (ECG). 2007. *Ecological Regions for the Northwest Territories – Taiga Plains*, Department of Environment and Natural Resources, Government of the Northwest Territories, Yellowknife, NT.

Ecosystem Classification Group (ECG). 2008. Ecological Regions for the Northwest Territories – Taiga Shield, Department of Environment and Natural Resources, Government of the Northwest Territories, Yellowknife, NT.

Hall, D.K. and Roswell C. 1981. The origin of water feeding icings on the eastern North Slope of Alaska, *Polar Record*, 20: 433-438.

Hall, D.K., Riggs, G.A. and Salomonson, V.V. 1995. Development of methods for mapping global snow cover using Moderate Resolution Imaging Spectroradiometer (MODIS) data, *Remote Sensing of Environment*, 54: 127-140.

Heginbottom, J.A., Dubreuil, M.A. and Harker, P.A. 1995. Canada-Permafrost, in *National Atlas of Canada, 5th ed., MCR 4177*, National Atlas Information Service, Natural Resources Canada, Ottawa, ON.

Kane, D.L. 1981. Physical mechanics of aufeis growth, Canadian Journal of Civil Engineering, 8: 186-195.

Kerr, D.E. and Wilson, P. 2000. Preliminary surficial geology studies and mineral exploration considerations in the Yellowknife area, Northwest Territories, Natural Resources Canada, *Geological Survey of Canada, Current Research 2000-C3*, Natural Resources Canada, Geological Survey of Canada, Ottawa, ON.

Morse, P.D. and Wolfe S.A. 2014. Icings in the Great Slave Region (1985–2014), Northwest Territories, Mapped from Landsat Imagery, *Geological Survey of Canada, Open File 7720*, Natural Resources Canada, Geological Survey of Canada Ottawa, ON.

Morse P.D., Wolfe S.A., Kokelj S.V. and Gaanderse A.J.R. In press. The occurrence and thermal disequilibrium state of permafrost in forest ecotopes of the Great Slave region, Northwest Territories, Canada. Permafrost and Periglacial Processes.

Romanovskii, N.N., Gravi, G.F., Melniko, E.S. and Leibman. M.O. 1996. Periglacial processes as geoindicators in the cryolithozone, in *Geoindicators: Assessing Rapid Environmental Changes in Earth Systems*, Berger, A.R. and Iams, W.J. (eds.), Balkema, Rotterdam, Netherlands: 47-67.

Spence, C. and Rouse, W.R. 2002. The energy budget of subarctic Canadian Shield subarctic terrain and its impact on hillslope hydrological processes, *Journal of Hydrometeorology*, 3: 208-218

Spence, C. and Woo, M.-K. 2003. Hydrology of subarctic Canadian Shield: soil filled valleys, Journal of Hydrology, 279: 151–166.

Spence, C., Kokelj, S.V. and Ehsanzadeh, E. 2011. Precipitation trends contribute to streamflow regime shifts in northern Canada, in *Cold Region Hydrology in a Changing Climate, Proceedings of symposium H02 held at Melbourne, Australia, July 2011, Publication 346*, Yang, D., Marsh, P., and Gelfan, A. (eds.), International Association of Hydrological Sciences, Oxfordshire, UK: 3-8.

Spence, C., Kokelj, S.A., Kokel, S.V. and Hedstrom, H. 2014. The process of winter streamflow generation in a subarctic Precambrian Shield catchment, *Hydrological Processes*, 28: 4179-4190.

Stevens, C.S., Kerr, D.E., Wolfe, S.A. and Eagles, S. 2012. Predictive surficial materials and geology derived from LANDSAT 7, Yellowknife, NTS 85J, Northwest Territories, *Geological Survey of Canada, Open File 7108*, Natural Resources Canada, Geological Survey of Canada, Ottawa, ON.

Veillette, J.J. and Thomas. R.D. 1979. Icings and seepage in frozen glaciofluvial deposits, District of Keewatin, N.W.T., *Canadian Geotechnical Journal*, 16: 789-798.

Yoshikawa, K., Petrone, K., Hinzman, L.D. and Bolton, W.R. 1999. Aufeis development and stream baseflow hydrology in the discontinuous permafrost region, Caribou Poker Creek Research Watershed, Interior Alaska, in *Program and Abstracts, 50th Arctic Science Conference, American Association for the Advancement of Science*, 19-22 September 1999, Denali National Park and Preserve, Alaska, American Association for the Advancement of Science Arctic Division, Fairbanks, AK, USA: 202-203.

Yoshikawa, K., Hinzman, L.D. and Kane, D.L. 2007. Spring and aufeis (icing) hydrology in Brooks Range, Alaska, *Journal of Geophysical Res*earch, 112: G04S43.